

INFRARED THERMAL WAVE STUDIES OF COMPOSITES

T. Ahmed, H.J. Jin, X. Wang, L.D. Favro, P.K. Kuo, and R.L. Thomas
Department of Physics and Institute for Manufacturing Research
Wayne State University
Detroit, Michigan 48202

INTRODUCTION

Thermal wave techniques have received increasing attention for use in the inspection and characterization of composite materials. These techniques have the advantages of being contactless, rapid requiring access to only one surface of the object under inspection. In this paper we demonstrate the ability of the technique to image flaws in several types of composite materials and to measure the depths of the flaws.

Our infrared thermal wave imaging system [1-3] consists of an infrared camera and a real-time image processor under the control of a computer workstation. A bank of up to eight xenon flash lamps, each 6 kJ energy and 2 ms pulse duration, are synchronously pulsed to launch thermal waves into the target from its surface. The IR camera is used to record the 8 μm to 12 μm infrared emission from the surface at a delay time corresponding to that required for the thermal waves to scatter back to the surface from the sub-surface defects of interest. Real-time image processing techniques and averaging are used to enhance the subsurface selectivity of the defect detection. Post processing of the data can also be utilized to achieve further improvements in the signal to noise ratio and image contrast.

EXPERIMENTAL

A block diagram of the experimental set-up is shown in Fig. 1. The system consists of an IR video camera (Inframetrics IR 600), a real-time image processor (Datacube), a computer workstation (Sun 3/160C), and up to eight flash heating units (Balcar-Starflash 3) with their associated electronic controls. For the measurements on the composite materials presented in this paper, the thermal wave time scales are such that a single video field can be considered to be instantaneous. It is thus sufficient to process the video images field-by-field as a function of time following a given heating pulse. All of the data processing takes place during the blanking time between the fields and frames, so as to preserve the quantitative accuracy of the time dependence. The procedure is repeated for N heating pulses (typically 8) and the resultant data are accumulated (averaged) in the image buffer. The mode of operation of the IR thermal wave imager is to produce series of synchronized, averaged images of the surface temperature distribution at various delay times following the heating pulse (and hence containing thermal wave reflections from various subsurface depths). To obtain such thermal wave reflection images, the incoming video data are accumulated in an image buffer only during a pre-set time-delayed ("box-car gate") window of time, with averaging over repetitive heating cycles to achieve the desired box-car integration, pixel-by-pixel. Our system allows the grabbing of an image, or a portion of an image, in up to four different gate time windows, each with different time delays after the heating pulse. The settings for these time delays are determined by observing the thermal

response curves of both a defective and a non-defective region of the sample, and are chosen to give the maximum contrast in the thermal wave image of a particular subsurface feature of interest. Images accumulating in the various image buffers for various gate delay times are combined arithmetically (i.e. added, subtracted, divided, etc.) in the fast video processor in such a way as to minimize time-independent background variations, e.g. to remove image artifacts resulting from spatial variations in the thermal emissivity of the sample surface. The processed images are accumulated over a number of repetitions (typically 16) of the heating pulse so as to improve the signal-to-noise ratio in the final digital image. The final image is subsequently post-processed in the Sun Workstation, where a variety of pseudocolor maps, filtering, line scans, perspective plot routines, etc. are utilized.

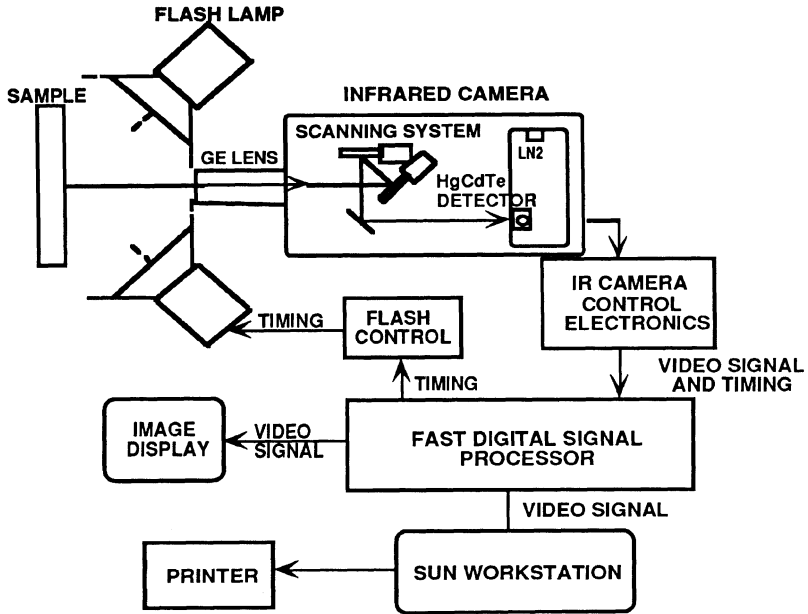


Fig. 1. A block diagram of the IR thermal wave imaging system.

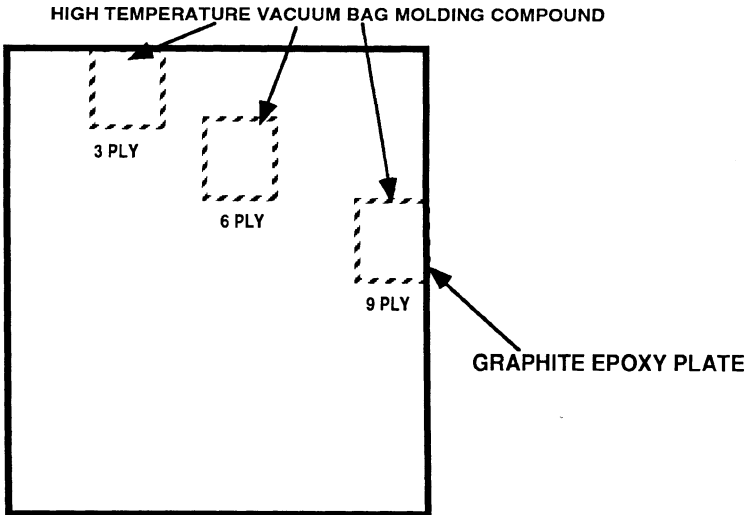


Fig. 2. A schematic diagram of a graphite/epoxy plate sample with inclusions.

RESULTS AND DISCUSSION

Figure 2 shows a schematic diagram of a graphite/epoxy composite plate with three rectangular inclusions at various depths. The inclusion is a polymer material used as high temperature vacuum bag molding sheet. The three inclusions were located at depths of 3, 6, and 9 plies beneath the sample surface. A thermal wave image (Fig. 3) at a gate time delay of 400 ms shows only the inclusion at the 3 ply depth. Figure 4, which is a thermal wave image at 833 ms, shows both the first (3 ply depth) and the second (6 ply depth) inclusions. In this sample there is insufficient image contrast at a single gate time to display simultaneously all three inclusions in the reflection mode. In Fig. 5, we show a transmission thermal wave image of the graphite/epoxy plate sample at 867 ms. It should be noted that, as expected, the inclusions in the transmission mode appear to be cooler than the background in contrast to the reflection mode images, in which they appear hotter.

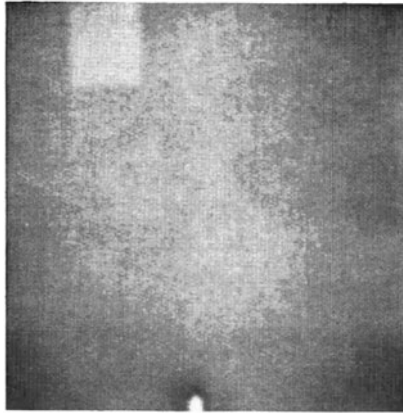


Fig. 3. Thermal wave image of graphite/epoxy plate at gate time delay of 400 ms showing the first inclusion.

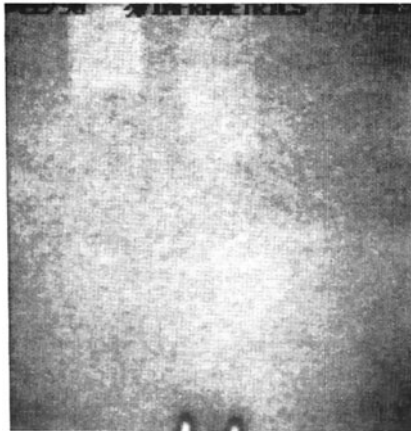


Fig. 4. Thermal wave image of graphite/epoxy plate at gate time delay of 833 ms showing the first and the second inclusions.

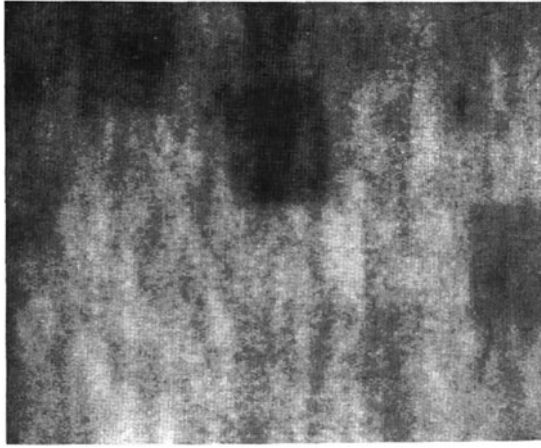


Fig. 5. Thermal wave image of graphite/epoxy plate at gate time delay of 867 ms showing the three inclusions in transmission mode.

The next set of illustrative images are of a graphite/epoxy composite sample with impact damage. At a short gate time (67 ms), the thermal wave image (Fig. 6) shows only the fibers in the first two plies nearest the surface (-45° ; 90°). At a somewhat longer gate time (167 ms, Fig. 7) there is some indication of the third ply ($+45^\circ$), and the impact damage area just begins to show up in the center of the image. At a much longer gate time (500 ms), the thermal wave image (Fig. 8) shows the impact damage area very clearly.

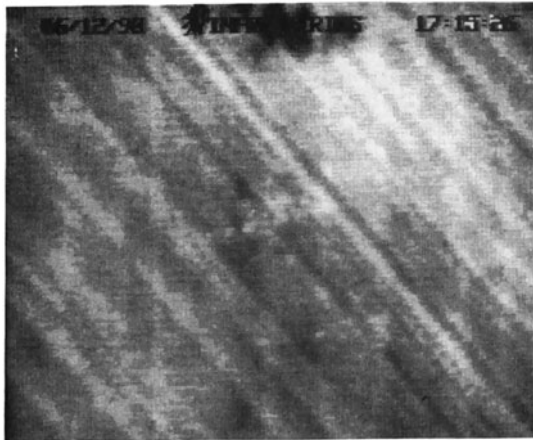


Fig. 6. Thermal wave image (gate time delay of 67 ms) of a graphite/epoxy impact damage specimen.

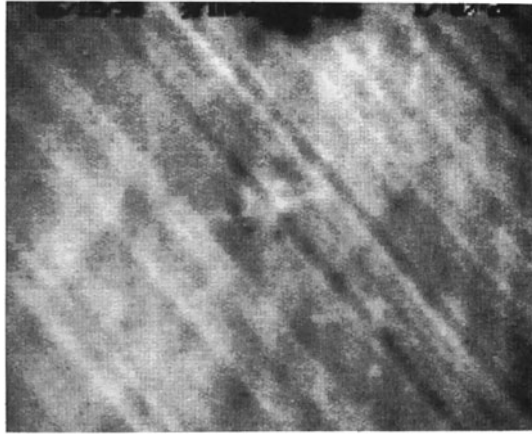


Fig. 7. Thermal wave image (gate time delay of 167 ms) of a graphite/epoxy impact damage specimen.

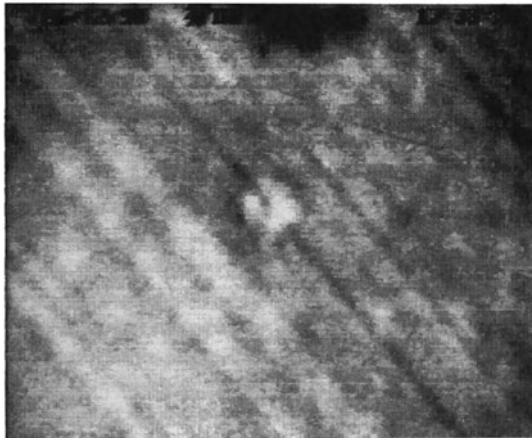


Fig. 8. Thermal wave image (gate time delay of 500 ms) of a graphite/epoxy impact damage specimen.

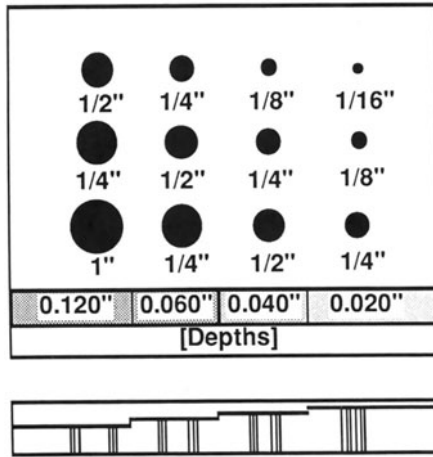


Fig. 9. Schematic diagram of a graphite/epoxy flat bottom hole/step test specimen.

A schematic diagram of a graphite/epoxy composite with twelve flat bottom holes and four steps is shown in Fig. 9. A thermal wave image (Fig. 10) of the flat bottom holes at a gate time of 3 sec shows the shallowest nine holes. In Fig. 11, the thermal wave image at a gate time delay of 12 sec. shows only the deepest nine holes, since the response from the shallowest holes has decayed. Finally, in Fig. 12, we show a thermal wave image of the step region of the test specimen at a gate time of 3 sec.

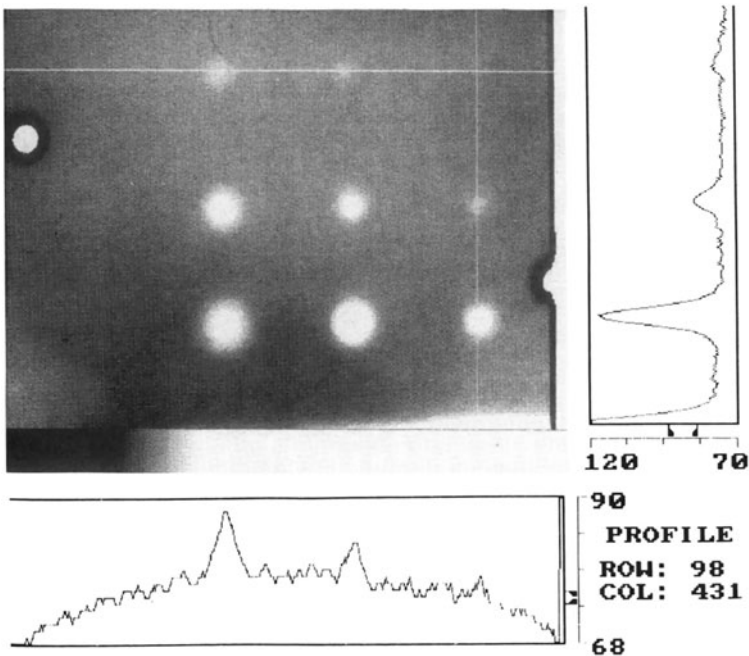


Fig. 10. Thermal wave image of the flat bottom hole sample at a gate time delay of 3 sec, with the shallowest nine holes being most easily discerned.

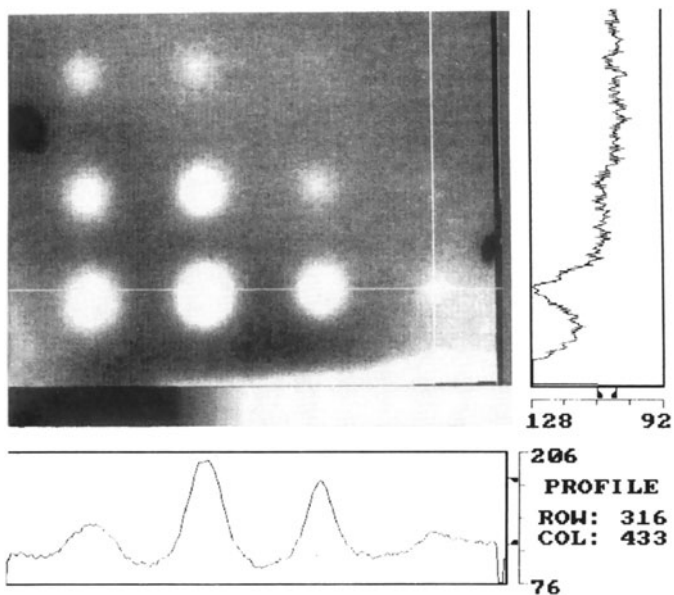


Fig. 11. Thermal wave image of the flat bottom hole sample at a gate time delay of 12 sec, with the deepest nine holes being most easily discerned.

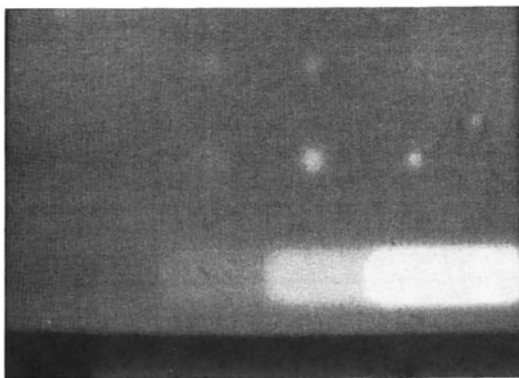


Fig. 12. Thermal wave image of the step area of the test sample at a gate time delay of 3 sec.

ACKNOWLEDGEMENTS

This work was sponsored by the Army Research Office, under Contract No. DAAL 03-88-K-0089 and by the Institute for Manufacturing Research, Wayne State University.

REFERENCES

1. P.K. Kuo, T. Ahmed, H.J. Jin, L.D. Favro, and R.L. Thomas, *Journal of NDE*, 8(2), 97 (1989).
2. P.K. Kuo, T. Ahmed, L.D. Favro, H.J. Jin, and R.L. Thomas, *Review of Progress in Quantitative NDE*, 8B, 1305, Plenum Press, New York (1989).
3. T. Ahmed, Z.J. Feng, P.K. Kuo, J. Hartikainen, and J. Jaarinen, *Journal of NDE*, 6(4), 190 (1987).